Supporting Material for:

Nuclear Inelastic Scattering and Mössbauer Spectroscopy as Local Probes for Ligand Binding Modes and Electronic Properties in Proteins: Vibrational Behavior of a Ferriheme Center Inside a β-Barrel Protein

Beate Moeser,[‡] Adam Janoschka,[‡] Juliusz A. Wolny,[‡] Hauke Paulsen,[†] Igor Filippov,[‖] Robert E. Berry,[‖] Hongjun Zhang,[‖] Alexander I. Chumakov,[#] F. Ann Walker,*[‖] and Volker Schünemann*[‡]

Full Author list of Reference 121:

121. Frisch, H.J.; Trucks, G.W.; Schlegel, H.B.; Scuseria, G.E.; Robb, M.A.; Cheeseman, J.R.; Montgomery, Jr., J.A.; Vreven, T.; Kudin, K.N.; Burant, J.C.; Millam, J.M.; Iyengar, S.S.; Tomasi, J.; Barone, V.; Mennucci, B.; Cossi, M.; Scalmani, G.; Rega, N.; Petersson, G.A.; Nakatsuji, H.; Hada, M.; Ehara, M.; Toyota, K.; Fukuda, R.; Hasegawa, J.; Ishida, M.; Nakajima, T.; Honda, Y.; Kitao, O.; Nakai, H.; Klene, M.; Li, H.; Knox, J.E.; Hratchian, H.P.; Cross, J.B.; Bakken, V.; Adamo, C.; Jaramillo, J.; Gomperts, R.; Stratmann, E.E.; Yazyev, O.; Austin, A.J.; Cammi, R.; Pomelli, C.; Ochterski, J.W.; Ayala, P.Y.; Morokuma, K.; Voth, G.A.; Salvador, P.; Dannenberg, J.J.; Zakrzewski, V.G.; Dapprich, S.; Daniels, A.D.; Strain, M.C.; Farkas, O.; Malick, D.K.; Rabuck, A.D.; Raghavachari, K.; Foresman, J.B.; Ortiz, J.V.; Cui, Q.; Baboul, A.G.; Clifford, S.; Cioslowski, J.; Stefanov, B.B.; Liu, G.; Liashenko, A.; Piskorz, P.; Komaromi, I.; Martin, R.L.; Fox, D.J.; Keith, T.; Al-Laham, M.A.; Peng, C.Y.; Nanayakkara, A.; Challacombe, M.; Gill, P.M.W.; Johnson, B.; Chen, W.; Wong, M.W.; Gonzalez, C.; and Pople, J.A.;. Gaussian 03, Revision E.01. Gaussian, Inc., Wallingford, CT, 2004.

Table S1. Structural parameters of the iron-ligand-bond in the optimized molecular structures of NP2 on which the calculations of the DOS presented in Figures 9-11 are based and corresponding iron ligand modes.

	Fe-Ligand distance [Å]	Fe-Ligand angle [°]	Fe-Ligand vibrations [cm^{-1}]
NP2-NO	1.639	179.9	Fe-NO-stretch (666), Fe-N-O-bend (598, 588)
NP2-CN	1.935	179.8	Fe-CN-stretch (464), Fe-C-N-bend (439)
NP2-Im	2.003		

Table S2. Frequency of calculated normal modes below 100 cm^{-1} with a mode composition factor e^2 >0.0001 as obtained from the QM/MM calculations of NP2-NO with the heme propionates doubly protonated and of NP2-CN and NP2-His with the heme propionates deprotonated

NP2-NO		**NP2-CN**		**NP2-His**	
Frequency [cm^{-1}]	e^2	Frequency [cm^{-1}]	e^2	Frequency [cm^{-1}]	e^2
17.498	0.0042	12.410	0.0029	21.116	0.0080
35.610	0.0041	83.083	0.0027	29.102	0.0053
70.290	0.0035	73.677	0.0026	38.778	0.0043
29.434	0.0033	47.179	0.0025	13.210	0.0040
72.290	0.0033	20.750	0.0024	29.933	0.0033

71.989	0.0032	35.242	0.0024	85,504	0.0028
68.645	0.0030	76.022	0.0024	66.196	0.0027
58.182	0.0027	13.315	0.0022	41.630	0.0026
37.954	0.0026	64.325	0.0021	44.440	0.0026
28.915	0.0025	72.665	0.0021	24.746	0.0025
11.393	0.0024	58.386	0.0020	27.725	0.0025
39.571	0.0024	58.852	0.0020	28.773	0.0025
16.168	0.0023	69.943	0.0020	29.128	0.0025
34.010	0.0023	71.589	0.0020	30.020	0.0025
37.125	0.0023	50.683	0.0019	21.945	0.0024
63.745	0.0022	60.782	0.0019	25.231	0.0024
72.161	0.0022	46.989	0.0018	30.274	0.0024
58.435	0.0020	50.829	0.0018	81.300	0.0022
70.214	0.0020	52.317	0.0018	86.709	0.0021
85.774	0.0020	53.717	0.0018	95.340	0.0021
60.175	0.0019	7.786	0.0017	72.350	0.0020
60.449	0.0019	15.130	0.0017	77.022	0.0020
60.755	0.0019	15.630	0.0017	87.317	0.0020
18.894	0.0018	23.715	0.0017	90.385	0.0020
48.038	0.0018	24.114	0.0017	61.343	0.0019
63.461	0.0018	34.043	0.0017	64.928	0.0019
14.780	0.0017	41.932	0.0017	65.101	0.0019
18.390	0.0017	43,532	0.0017	69.136	0.0019
18.559	0.0017	48.451	0.0017	75.370	0.0019
19.451	0.0017	49.306	0.0017	84.254	0.0019
19.480	0.0017	51.461	0.0017	91.966	0.0019

19.756	0.0017	10.710	0.0016	18.025	0.0018
20.891	0.0017	12.724	0.0016	19.692	0.0018
21.274	0.0017	15.296	0.0016	32.716	0.0018
21.418	0.0017	19.208	0.0016	35.072	0.0018
21.678	0.0017	19.911	0.0016	36.549	0.0018
21.978	0.0017	21,474	0.0016	36.977	0.0018
33.529	0.0017	21.591	0.0016	37.359	0.0018
36.149	0.0017	22.292	0.0016	37.715	0.0018
39.423	0.0017	23.109	0.0016	38.625	0.0018
39.817	0.0017	24,674	0.0016	40.755	0.0018
41.304	0.0017	25.387	0.0016	42.449	0.0018
44.971	0.0017	25.665	0.0016	46.144	0.0018
46.513	0.0017	26.335	0.0016	46.400	0.0018
47.322	0.0017	26.938	0.0016	48.128	0.0018
47.569	0.0017	26.991	0.0016	50.065	0.0018
49.952	0.0017	27.451	0.0016	50.816	0.0018
58.745	0.0017	29.435	0.0016	51.080	0.0018
6.094	0.0016	29.856	0.0016	53.344	0.0018
13.393	0.0016	31.669	0.0016	55.651	0.0018
13.477	0.0016	32.605	0.0016	55.916	0.0018
14.477	0.0016	33.867	0.0016	56.839	0.0018
16.319	0.0016	34,538	0.0016	68.761	0.0018
22.660	0.0016	36.256	0.0016	73.020	0.0018
22.895	0.0016	39.882	0.0016	87.396	0.0017

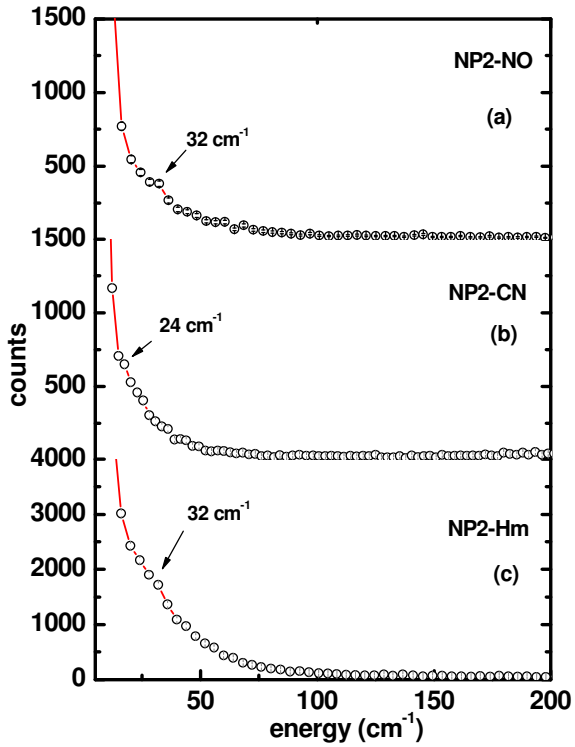

Figure S1: Low-energy region of the NIS spectra displayed in Fig. 1 of the text, with indicated peaks at very low energies.

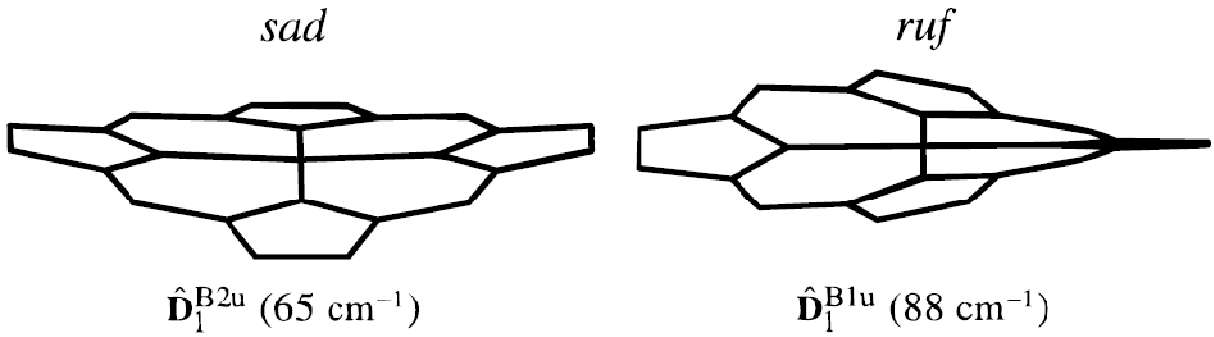

Figure S2. Schematic representation of a saddling (sad, B_{2u}) and ruffling (ruf, B_{1u}) mode of a porphyrin ring with ideal D_{4h} symmetry. The graphic is taken from Jentzen et al.[S1]

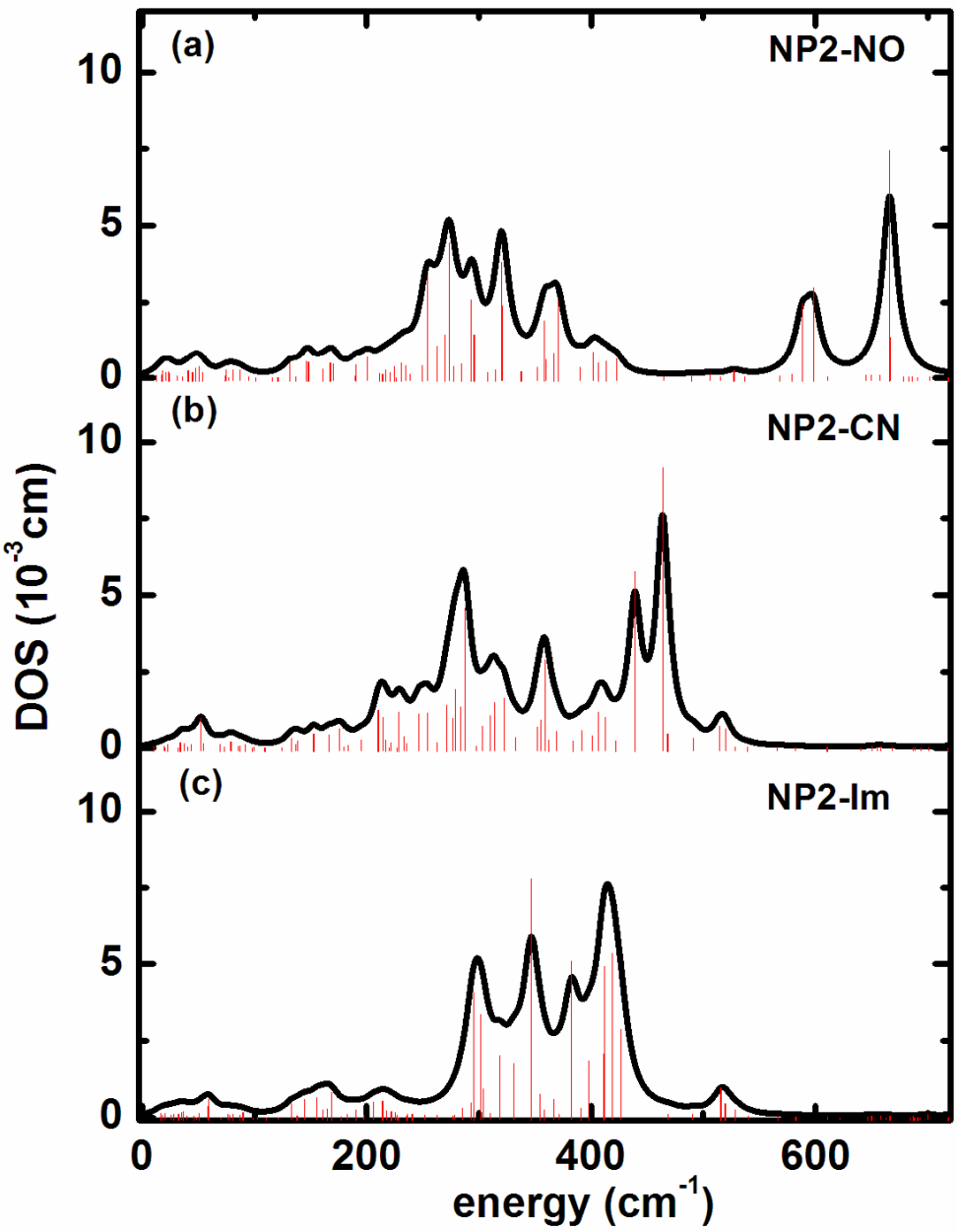

Figure S3. Iron vibrational density of states calculated on the basis of the optimized molecular structures of the isolated heme complexes shown in figure 7a-c. The bar graphs display the mode composition factor e^2, normalized such that the highest value in each graph is 0.06.

Reference

S1. Jentzen, W.; Song, X.; Shelnutt, J. A. *J. Phys. Chem. B.* **1997**, *101*, 1684-1699.

13 Movies are attached below in one zipped folder. To open these movies, use your favorite web browser.

Mov1_NP2_NO_630.gif

Normal mode at 630 cm^{-1} for NP2-NO calculated using the ONIOM approach and protonated heme carboxylates, only the layer calculated by DFT is shown.

Mov2_NP2_NO_591.gif

Normal mode at 591 cm^{-1} for NP2-NO calculated using the ONIOM approach and protonated heme carboxylates, only the layer calculated by DFT is shown.

Mov3_NP2_NO_582.gif

Normal mode at 582 cm^{-1} for NP2-NO calculated using the ONIOM approach and protonated heme carboxylates, only the layer calculated by DFT is shown.

Mov4_NP2_NO_70.gif

Normal mode at 70 cm^{-1} for NP2-NO calculated using the ONIOM approach and protonated heme carboxylates.

Mov5_NP2_NO_17.gif

Normal mode at 17 cm^{-1} for NP2-NO calculated using the ONIOM approach and protonated heme carboxylates.

Mov6_NP2_CN_455.gif

Normal mode at 455 cm^{-1} for NP2-CN calculated using the ONIOM approach and deprotonated heme carboxylates, only the layer calculated by DFT is shown.

Mov7_NP2_CN_451.gif

Normal mode at 451 cm^{-1} for NP2-CN calculated using the ONIOM approach and deprotonated heme carboxylates, only the layer calculated by DFT is shown.

Mov8_NP2_CN_83.gif

Normal mode at 83 cm^{-1} for NP2-CN calculated using the ONIOM approach and deprotonated heme carboxylates.

Mov9_NP2_CN_12.gif

Normal mode at 12 cm^{-1} for NP2-CN calculated using the ONIOM approach and deprotonated heme carboxylates.

Mov10_NP2_Im_422.gif

Normal mode at 422 cm^{-1} for NP2-Im calculated using the ONIOM approach and deprotonated heme carboxylates, only the layer calculated by DFT is shown.

Mov11_NP2_Im_389.gif

Normal mode at 389 cm^{-1} for NP2-Im calculated using the ONIOM approach and deprotonated heme carboxylates, only the layer calculated by DFT is shown.

Mov12_NP2_Im_383.gif

Normal mode at 383 cm^{-1} for NP2-Im calculated using the ONIOM approach and deprotonated heme carboxylates, only the layer calculated by DFT is shown.

Mov13_NP2_Im_21.gif

Normal mode at 21 cm^{-1} for NP2-Im calculated using the ONIOM approach and deprotonated heme carboxylates.